Involvement of an ABC Transporter in a Developmental Pathway Regulating Hypocotyl Cell Elongation in the Light

Michael Sidler,[1] Paul Hassa,[1] Sameez Hasan, Christoph Ringli, and Robert Dudler[2]

Institute of Plant Biology, University of Zurich, Zollikerstrasse 107, CH-8008 Zurich, Switzerland

In the dark, plant seedlings follow the skotomorphogenetic developmental program, which results in hypocotyl cell elongation. When the seedlings are exposed to light, a switch to photomorphogenetic development occurs, and hypocotyl cell elongation is inhibited. We have manipulated the expression of the *AtPGP1* (for *Arabidopsis thaliana* P glycoprotein1) gene in transgenic Arabidopsis plants by using sense and antisense constructs. We show that within a certain light fluence rate window, overexpression of the *AtPGP1* gene under the control of the cauliflower mosaic virus 35S promoter causes plants to develop longer hypocotyls, whereas expression of the gene in antisense orientation results in hypocotyls shorter than those occurring in the wild type. In the dark, hypocotyls of transgenic and wild-type plants are indistinguishable. Because the *AtPGP1* gene encodes a member of the superfamily of ATP binding cassette–containing (ABC) transporters, these results imply that a transport process is involved in a hypocotyl cell elongation pathway active in the light. The AtPGP1 transporter is localized in the plasmalemma, as indicated by immunohistochemical techniques and biochemical membrane separation methods. Analysis of the *AtPGP1* expression pattern by using reporter gene constructs and in situ hybridization shows that in wild-type seedlings, *AtPGP1* is expressed in both the root and shoot apices.

INTRODUCTION

A young seedling's predominant endeavor is to reach favorable light conditions to switch from heterotrophic to photoautotrophic growth. Consequently, light, which serves as energy source, provides important information for plant morphogenesis. Plants make use of a sophisticated system of photoreceptors to sense the quality, quantity, periodicity, and direction of light (Kendrick and Kronenberg, 1994). At least three different photoreceptor systems are known to be involved in modulating development: phytochromes, which primarily absorb red and far-red light; blue light/UV-A receptors; and UV-B receptors (Chamovitz and Deng, 1995; Quail et al., 1995). Depending on the light conditions, seedlings can follow two developmental programs. In darkness, their hypocotyls elongate, the yellow cotyledons are kept closed, and apical hooks are formed (skotomorphogenesis). On the other hand, light triggers deetiolation, which results in inhibition of hypocotyl elongation, opening of apical hooks, unfolding of the cotyledons, and development of chloroplasts (photomorphogenesis). Recently, mutations at the *PROCUSTE1* locus that cause specific defects in hypocotyl cell elongation in dark-grown plants have been described in Arabidopsis (Desnos et al., 1996). The observation that light stimulates hypocotyl cell elongation in these mutant seedlings uncovered a novel *PROCUSTE1*-independent genetic pathway termed X that controls hypocotyl cell elongation in dim light (Desnos et al., 1996).

We previously cloned the multidrug resistance (*MDR*)–like gene *AtPGP1* (for *Arabidopsis thaliana* P glycoprotein1) from Arabidopsis (Dudler and Hertig, 1992). The products of *MDR*-like genes belong to the ubiquitously occurring family of ATP binding cassette–containing (ABC) transporters that mediate the ATP-driven transmembrane translocation of a large variety of substrates (Higgins, 1992; Gottesman et al., 1995). To analyze the function of *AtPGP1*, we manipulated its expression in transgenic plants. Here, we present evidence that AtPGP1 is involved in a hypocotyl cell elongation program that is active in dim light, thus implicating a transport function in this developmental process. Localization experiments and analysis of the *AtPGP1* expression pattern indicated that AtPGP1 is localized in the plasma membrane and that the corresponding gene is expressed in both the root and shoot apices of seedlings.

RESULTS

Generation and Analysis of Transgenic Arabidopsis Plants Constitutively Expressing *AtPGP1* Gene Constructs in Sense and Antisense Orientations

To analyze the function of the *AtPGP1* gene, we generated two series of transgenic Arabidopsis plants. Plants of the first series expressed the *AtPGP1* gene constitutively under the control of the cauliflower mosaic virus (CaMV) 35S

[1] These authors contributed equally to this work.
[2] To whom correspondence should be addressed. E-mail rdudler@botinst.unizh.ch; fax 41-1-634-82-04.

promoter. In the second series, the suppression of AtPGP1 protein synthesis was attempted by constitutive expression of an antisense construct driven by the same promoter. The constructs were introduced into the Arabidopsis genome by using the Agrobacterium-mediated in-the-plant transformation system (Bechtold et al., 1993). Plants from the first six independently transformed lines homozygous for the 35S-AtPGP1 gene (OE lines) and the first five lines homozygous for the antisense construct (AS lines) were analyzed in the T$_3$ generation. RNA gel blot analysis showed that in all OE lines, AtPGP1-specific mRNA of ~4.5 kb was much more abundant than in nontransformed wild-type plants (Figures 1A and 1B). In the AS lines, new RNA of the expected length of 1.9 kb as well as shorter fragments could be detected with a double-stranded AtPGP1-specific hybridization probe, whereas in most cases, the authentic mRNA of 4.5 kb was less abundant than in the wild type.

The transgene-mediated modification of AtPGP1 expression could be confirmed at the protein level. Figures 1C and 1D show gel blots of microsomal membrane proteins probed with an AtPGP1-specific rabbit antiserum raised against a fusion protein produced in Escherichia coli. In extracts from OE plants, the antibody identified a single band of ~140 kD (Figure 1C). This is in good agreement with the theoretically calculated weight of 140.57 kD for AtPGP1. No signal was detected in the lane with proteins extracted from wild-type plants on this blot, which contained 10 μg of protein per lane, indicating that in wild-type plants, AtPGP1 is not an abundant protein. However, when 100 μg of protein was loaded per lane, the antibody detected two bands in extracts of wild-type plants in the size range of ~130 to 140 kD (Figure 1D).

In AS plants, both bands were visible as well, but in most cases, the upper one appeared to be reduced compared with the lower one (Figure 1D). To determine which of the two bands corresponded to AtPGP1, we co-electrophoresed membrane proteins from the AS2 line with an aliquot of OE3 protein (lane AS2/OE3 in Figure 1D). Because the upper band was enhanced by the addition of OE3 extract, it must represent AtPGP1, whereas the lower one most likely represents a cross-reacting homolog. The reduction of AtPGP1 in AS lines was quantified densitometrically by using the lower band as an internal standard. Figure 1E shows that the amount of AtPGP1 in the AS plants reached 30 to 80% of the wild-type level, depending on the individual transgenic line. These values may overestimate AtPGP1 levels in AS plants because it is possible that the upper band represents additional cross-reacting proteins. Thus, the antisense strategy to knock out AtPGP1 expression had worked at least in part. For OE plants, the amount of AtPGP1 was estimated to be enhanced above that of the wild type by a factor of ~200.

AtPGP1 Mediates Hypocotyl Length in the Light

We observed that in comparison with the wild type, all six independently transformed OE lines used in this study exhib-

ited elongated hypocotyls, whereas AS plants had shorter ones. In Figure 2, the average hypocotyl length of all lines is plotted from germination of the seeds until maximal elongation of the hypocotyl. Under the growth conditions used in this experiment (an 18-hr photoperiod with 75 μmol m^{-2} sec^{-1} white light at 24°C), hypocotyls of AS, wild-type, and
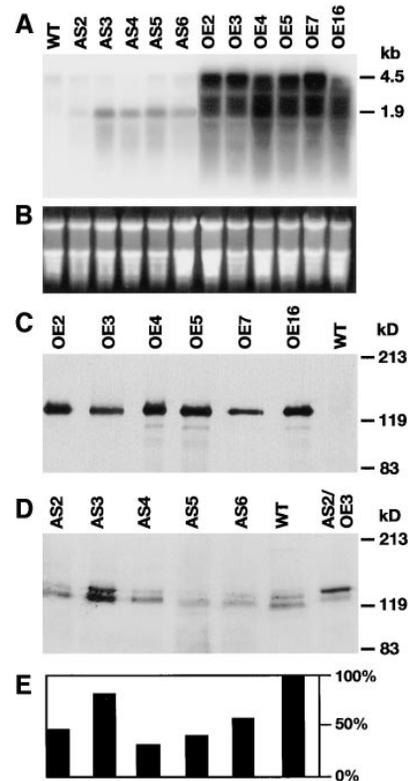

Figure 1. Analysis of AtPGP1 Expression in Wild-Type and Transgenic AS and OE Plants.

(A) Autoradiography of an RNA gel blot probed with a double-stranded ^{32}P-labeled probe. Each lane contains 8 μg of total RNA. The expected lengths of AtPGP1 and antisense transcripts are 4.5 and 1.9 kb, respectively. The lengths in kilobases of marker fragments are indicated at right. WT, wild type.
(B) Ethidium bromide–stained gel before blotting.
(C) and **(D)** Gel blot analysis of membrane proteins extracted from OE, AS, and wild-type plants. Ten and 100 μg of microsomal proteins were loaded per lane on the gels corresponding to the blots shown in **(C)** and **(D)**, respectively. The lane labeled AS2/OE3 in **(D)** contained 100 μg of AS2 and 2 μg of OE3 microsomal proteins. The blots were probed with an AtPGP1-specific rabbit antiserum and processed with the ECL chemiluminescent detection system. The sizes of the marker proteins are given at right in kilodaltons.
(E) Relative intensities of the upper band (corresponding to AtPGP1) to the lower band (serving as an internal standard) in corresponding lanes in **(D)**. The histogram represents the percentage values of this ratio relative to the wild type.
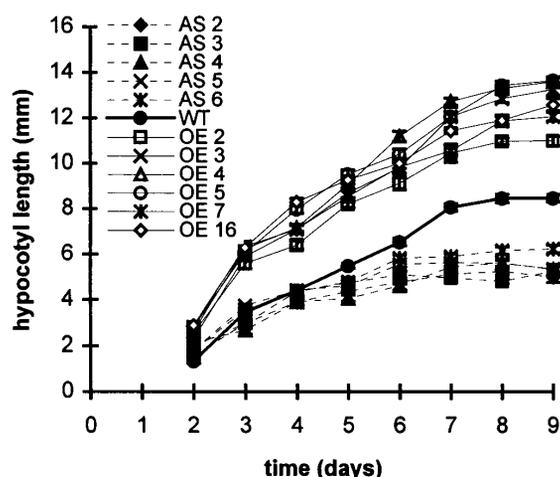
Figure 2. Analysis of the Hypocotyl Growth Rate of Wild-Type and Transgenic Plants.

The plants were grown under long-day conditions (18-hr photoperiod at 24°C) under white light at a fluence rate of 75 μmol m^{-2} sec^{-1}. Each data point represents the average length of 10 to 25 plants. For the wild type (WT), 20 to 35 hypocotyls were measured per day. The error bars indicate the standard error of the mean.

OE plants reached maximal average lengths of ~5, 8, and 12 mm, respectively, 9 days after germination.

The difference in hypocotyl length of wild-type, OE, and AS plants in theory may be caused by an increase in cell elongation, cell number, or both. To determine which parameter was affected by the transgene, we counted epidermal cells in the files in which they were arranged in the hypocotyl (Gendreau et al., 1997). As is evident from Figure 3A, AS plants had shorter and OE plants longer epidermal cells in their hypocotyl than did the wild type, whereas the number of cells in each file was identical in transgenic and wild-type plants (Figure 3B).

The phenotypic effect of the transgenes on the hypocotyl length could only be observed in plants that were grown in the light. The hypocotyl lengths of etiolated AS, OE, and wild-type seedlings exhibited no statistically significant difference. The data shown in Figure 4A originated from three different experiments. Seedlings were grown in a dark-growth cabinet and collected in single experiments after 5, 7, and 8 days to ensure that hypocotyls had reached maximal length. Hypocotyl lengths reached maximal values after 5 days and were not significantly different in transgenic and wild-type plants (Student's t test and ANOVA test; 95% confidence level).

Because light quality has a major impact on a young seedling's hypocotyl length (von Arnim and Deng, 1994), the response of the transgenic plants to far-red, red, and blue light with defined spectra was investigated. As shown in Figures 4B to 4D, the relative differences of hypocotyl lengths

between the transgenic and wild-type plants remained qualitatively the same under all wavelengths. As previously described (Desnos et al., 1996), blue light inhibition of hypocotyl growth was stronger than the effect exerted by red light (Figures 4B and 4C). Interestingly, under red light, OE plants developed longer hypocotyls than they did in complete darkness (Figures 4A and 4B). Seedlings grown under red light showed the characteristic lack of negative gravitropism (Golan et al., 1996), indicating a bona fide red light response (data not shown). Under continuous far-red light, the seedlings remained very short (Figure 4D) and were deetiolated but never became green.

To determine the light dose response of transgenic and wild-type plants, we grew seedlings under different fluence rates of white light with a 6-hr night break, and maximal hypocotyl lengths were measured. As depicted in Figure 5, above a light fluence rate of ~0.5 μmol m^{-2} sec^{-1}, the hypocotyls of wild-type plants became longer with increasing
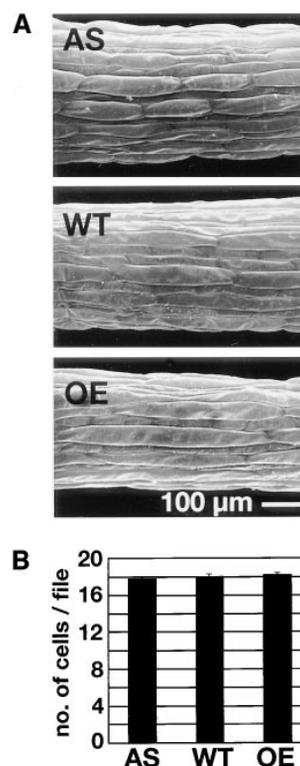

Figure 3. Number and Length of Hypocotyl Cells in 7-Day-Old Wild-Type, AS, and OE Plants Grown at a Light Fluence Rate of 52 μmol m^{-2} sec^{-1}.

(A) Scanning electron microscopy of hypocotyls.
(B) Number of epidermal cells per file in hypocotyls. Eight hypocotyls from each of two AS lines, two OE lines, and the wild type were scored. The error bars indicate the standard error of the mean. WT, wild type.
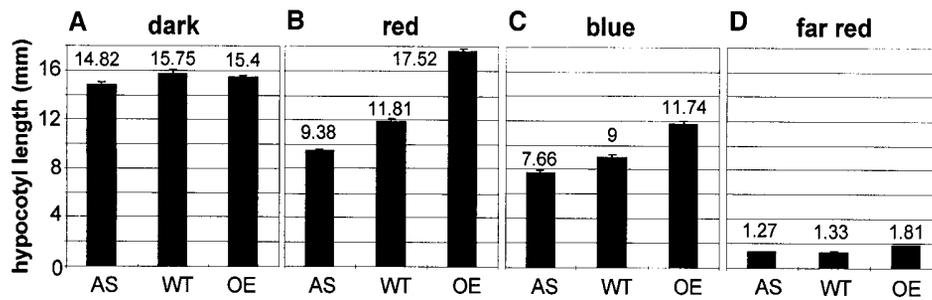
Figure 4. Influence of Light Quality on Hypocotyl Length in Wild-Type, AS, and OE Plants.

(A) Hypocotyl lengths of etiolated seedlings. The data represent the averages of three independent measurements conducted after 5, 7, and 8 days of growth in complete darkness. Hypocotyls already had reached maximal length after 5 days. A total of 142 AS and 190 OE seedlings of all transgenic lines and 102 wild-type seedlings were scored. The differences between OE, AS, and wild-type plants are statistically not significant at the 95% confidence level.

(B) to **(D)** Seedlings of two AS lines, two OE lines, and the wild type were grown in light of different qualities, and hypocotyls were measured at two different time points that yielded identical results, thus ensuring full elongation. In **(B)**, 40 seedlings per line were measured after 19 days of growth in red light at a fluence rate of 25 μmol m^{-2} sec^{-1}. In **(C)**, 20 seedlings per line were scored after 14 days in blue light at a fluence rate of 15 μmol m^{-2} sec^{-1}. In **(D)**, 18-day-old seedlings were grown under far-red light at a fluence rate of 2 μmol m^{-2} sec^{-1}. Twenty seedlings per line were scored.

Error bars indicate the standard error of the mean. WT, wild type.

light fluence rate and reached a maximal length at ~20 μmol m^{-2} sec^{-1}. Higher fluence rates resulted in shorter hypocotyls. The elongation of OE hypocotyls under dim light was greatly increased; in AS lines, it was essentially abolished. Hypocotyls in all lines decreased in length at higher light fluence rates and were indistinguishable at 100 μmol m^{-2} sec^{-1}, reaching a length of ~2 mm.

AtPGP1-Overexpressing Plants Have Longer Roots

As depicted in Figure 6, overexpression of *AtPGP1* also had a phenotypic effect on roots. Roots of OE plants grown on soil for 12 days under normal conditions (20 hr of light at a fluence rate of 75 μmol m^{-2} sec^{-1}) were slightly longer than the roots of wild-type and AS plants. The roots of the latter seemed to be shorter than those of the wild type, but in contrast to OE plants, the difference was not significant in statistical tests at a confidence level of 95%. Root length was also measured 8 days after germination with essentially the same results: OE roots were significantly longer than those of wild-type plants, whereas AS roots appeared to be slightly shorter, although the difference between AS and wild-type roots was statistically not significant (data not shown).

Apart from the hypocotyl and root phenotypes, no other phenotypic effect of the transgenes was observed in any OE and AS line throughout the complete life cycle of the plant. Because the products of *MDR*-like genes often are involved in resistance against toxic compounds and heavy metals (Ortiz et al., 1992; Gottesman et al., 1996), the transgenic plants also were tested for their tolerance to emetine and doxorubicine, two compounds known to induce multidrug

resistance in mammalian cells, as well as for their resistance to the herbicides paraquat, azifluorfen, atrazine, and alachlor and the heavy metal cadmium sulfate. No difference between AS, wild-type, and OE plants was detected (data not shown).

AtPGP1 Expression Pattern of Wild-Type Plants

To examine the expression pattern of the *AtPGP1* gene, we placed the β-glucuronidase (GUS)–encoding *uidA* gene from *E. coli* under the control of the *AtPGP1* promoter (2.1 kb of 5' flanking sequence). After the introduction of this reporter gene into the Arabidopsis genome, kanamycin-resistant plants from 16 independent transgenic lines were analyzed in the T_1 generation by histochemical detection of GUS activity. In seedlings of all 16 independent lines, staining of the shoot apex was observed, whereas root apices exhibited GUS activity in 12 of the 16 lines (Figures 7A to 7D). In the shoot apex of these 16 lines, the meristematic region, leaf primordia, and young leaves as well as the proximal regions of the vascular tissue of cotyledons and the hypocotyl were stained, whereas the remaining parts of these organs never exhibited any GUS activity. Staining first became visible in the shoot apex ~24 hr after germination. As leaves expanded with progressive age, staining largely disappeared in these organs. Only the proximal part of the midrib frequently showed (12 of 16) weak GUS staining in fully expanded rosette leaves (data not shown). In 12 of the 16 lines, the elongation zone and frequently the specialization zone of roots, including the first root hairs, were stained (Figure 7D). The same pattern was observed in lateral roots, in which GUS activity

could be detected very early after initialization from cells in the pericycle.

Plants of 13 independent lines also were examined at flowering stages (data not shown). In all lines, the most intense GUS activity was associated with the nodes of the stem, including the bases of cauline leaves, the proximal part of the midrib, and the secondary inflorescence meristematic regions. In six of the 13 lines, the receptacles of flowers were stained, whereas other flower parts never exhibited GUS activity. In one of the six lines showing staining of the receptacles, the nectaries exhibited particularly strong GUS activity. Because this was observed in only one line, its significance is unknown. In roots, blue coloring was never observed at root tips, in contrast to the pattern in seedlings, but sometimes GUS staining was visible in the stele of relatively indistinct parts of the root system near bifurcations. It is not clear whether the weak staining in these older plant parts reflects activity of the reporter gene or just GUS activity that remained stable.

The GUS staining pattern was also observed in reporter plants of several lines subjected to all experimental conditions used in experiments with OE, AS, and wild-type plants. No change in the GUS staining pattern was observed in any of the experiments, indicating that *AtPGP1* expression is seemingly independent of changes in the environmental conditions.

The *AtPGP1* gene expression pattern was also analyzed by in situ hybridization of whole-mount preparations of roots and of longitudinal sections through the hypocotyl and shoot apices of Arabidopsis seedlings before germination and 12, 24, 72, 96, and 120 hr after germination. As is evident from examples shown in Figures 7E to 7N, the results
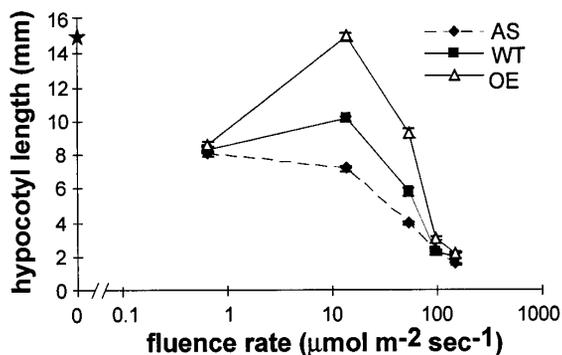

Figure 5. Influence of Light Quantity on Hypocotyl Length in Wild-Type, AS, and OE Plants.

Seedlings were grown under white light at different light fluence rates, and hypocotyls were measured at two different time points to ensure full elongation. The star on the vertical axis indicates the average hypocotyl length of etiolated seedlings (taken from the data presented in Figure 4). Data points represent measurements of 30 to 40 seedlings of the wild type (WT) and each of three AS and two OE lines, respectively. Error bars indicate the standard error of the mean.
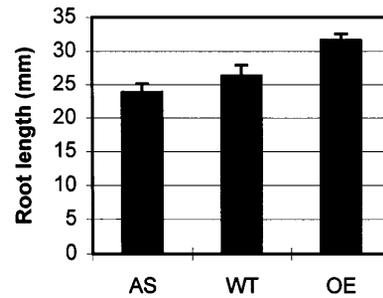

Figure 6. Root Length of Wild-Type, AS, and OE Seedlings.

Seedlings were grown on soil under white light at a fluence rate of 48 μmol m^{-2} sec^{-1}. Roots of two AS lines (30 seedlings), two OE lines (55 seedlings), and the wild type (WT; 19 seedlings) were scored after 12 days. Roots of OE plants were significantly different from those of AS and wild-type plants, whereas the difference between AS and wild-type roots was not statistically significant at the 95% confidence level. Error bars indicate the standard error of the mean.

of these experiments essentially confirmed the *AtPGP1* expression pattern inferred from the transgenic seedlings harboring the *GUS* reporter gene. Hybridization signals were not detected in longitudinal sections of vernalized seeds 12 hr after transfer to light and 24°C ambient temperature (Figures 7E and 7F) but appeared in the shoot apex and to a lesser extent in the cotyledons of seedlings 12 and 24 hr after germination, respectively (Figures 7G to 7J). Germination occurred 12 to 16 hr after transfer to normal growth conditions. In situ hybridization of longitudinal sections through hypocotyls of seedlings at any age never revealed a clear positive stain except for the region of the vascular strand most proximal to the apex (Figures 7K and 7L). The only slight divergence from the GUS staining pattern was found in roots, where in situ hybridization revealed a distinct signal at the region of the quiescent center (Figures 7M and 7N). In transgenic reporter plants, this region was not stained at all or was at the end of a decreasing gradient of GUS staining.

Subcellular Localization of AtPGP1

The subcellular localization of AtPGP1 as an integral membrane protein was examined by both immunohistochemical and biochemical techniques. Unfortunately, the polyclonal antibody raised against the AtPGP1 fusion protein was not suitable for immunohistochemical localization experiments because it unspecifically cross-reacted with tissue sections. Therefore, transgenic plants were generated harboring a modified CaMV 35S promoter–driven *AtPGP1* gene encoding a c-Myc epitope–tagged protein. The c-Myc epitope, which is recognized by the monoclonal antibody 9E10 (Evan et al., 1985), was introduced at position 1274 of the 1286–amino acid AtPGP1 protein. The construct was transferred
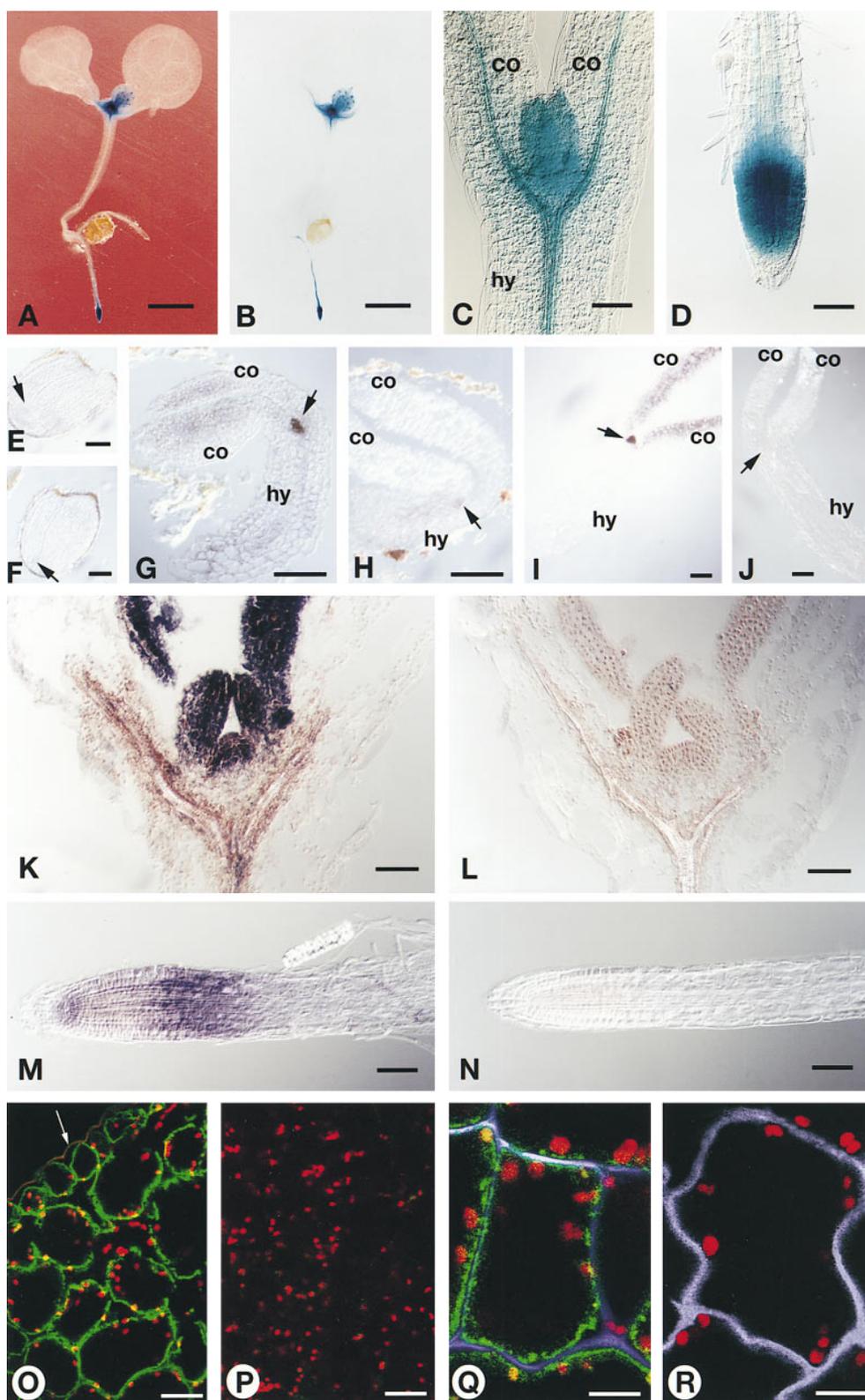
Figure 7. Localization of *AtPGP1* Gene Expression and of AtPGP1 Protein.

into the Arabidopsis genome by using the Agrobacterium-mediated transformation system. Hand-cut sections of homozygous transformants were fixed and probed with the anti–c-Myc antibody 9E10. To visualize bound antibody, we used a dichlorotriazynil aminofluorescein (DTAF)–conjugated secondary antibody.

Examination of immunostained leaf and meristem sections with a confocal laser scanning microscope revealed that the cells were exclusively labeled at the periphery, which is consistent with localization in the plasma membrane (Figures 7O and 7Q). Sections of wild-type control plants displayed no labeling, indicating that the signal very specifically represented the c-Myc epitope (Figures 7P and 7R). Experiments with transgenic plants expressing tagged AtPGP1 protein containing the c-Myc epitope at different positions (at Leu-14 near the N terminus and at Glu-80 in the first putative extracellular loop, respectively) revealed identical results (data not shown).

These results were confirmed by biochemical fractionation experiments. Microsomal membrane fractions were isolated from wild-type and transgenic plants expressing c-Myc epitope–tagged AtPGP1 and separated by continuous sucrose gradient centrifugation (Figures 8A and 8B). Gradient fractions were analyzed on protein gel blots. To determine the distribution of the different membrane compartments in the gradient, we used antibodies raised against VM23, a tonoplast protein (Maeshima, 1992); BiP, a protein localized in the lumen of the endoplasmic reticulum (Herman et al., 1994); and PIP, a plasmalemma protein (Kammerloher et al., 1994). As shown in Figure 8A, AtPGP1 from wild-type plants (detected with the AtPGP1-specific antiserum) and c-Myc epitope–tagged AtPGP1 from transgenic plants (detected with the 9E10 monoclonal antibody) migrated at the same positions in gradients run simultaneously. Both proteins comigrated with PIP, the plasmalemma marker protein, but

not with the vacuolar VM23 and the endoplasmic reticulum–localized BiP proteins, indicating a location in the plasma membrane. These results are in good agreement with the findings of the immunocytochemical studies and show that despite the ectopic expression and the epitope-tagging of AtPGP1, the intracellular targeting was not affected.

DISCUSSION

Manipulation of AtPGP1 Levels in Transgenic Plants

To study the function of the *AtPGP1* gene, we constitutively and ectopically expressed it by using transgenic Arabidopsis plants in both sense and antisense orientations under the control of the CaMV 35S promoter. RNA and protein gel blot analyses showed that OE plants of the six independent lines analyzed contained much higher levels of both *AtPGP1*-specific RNA and protein than did wild-type plants. On protein gel blots, the antiserum raised against the AtPGP1 fusion protein recognized two bands of ~130 to 140 kD in membrane protein extracts of wild-type plants. We could show that the higher band at 140 kD corresponds to the AtPGP1 protein by superimposing AS and OE membrane protein samples. The AtPGP1 levels found in membrane preparations of the AS lines were estimated to range between 30 and 80% of the wild-type value. Although these values may underestimate the true reduction achieved because the 140-kD band may also represent cross-reacting AtPGP1 homologs, it is likely that some residual AtPGP1 is still present in all lines. The rough estimates of AtPGP1 levels that were obtained are not well correlated with the observed phenotype of individual AS lines. It is conceivable

---

Figure 7. (continued).

(A) to (D) Histochemical localization of GUS activity in transgenic plants harboring an *AtPGP1–GUS* reporter gene. In (A) and (B), 7-day-old seedlings were photographed with two different background colors. In (C) and (D), the shoot and root apex, respectively, of a 5-day-old seedling are shown. In (A) and (B), bars = 1 mm; in (C) and (D), bars = 100 μm.

(E) to (N) Detection of *AtPGP1*-specific RNA by in situ hybridization in wild-type seedlings. In (E) to (L), longitudinal sections through seeds 12 hr after transfer from vernalization to growth conditions ([E] and [F]) and through seedlings 12 hr ([G] and [H]), 24 hr ([I] and [J]), and 5 days ([K] and [L]) after germination were hybridized with a digoxigenin-labeled *AtPGP1*-specific antisense RNA probe ([E], [G], and [I]) or with a sense RNA probe as a control ([F], [H], and [J]). In (M), a whole mount of a root of a 5-day-old seedling was hybridized with a digoxigenin-labeled antisense RNA probe. In (N), a section similar to the one shown in (M) was hybridized with a sense RNA probe as a control. Arrows indicate the shoot apex. Bars = 100 μm.

(O) to (R) Immunocytochemical localization of c-Myc epitope–tagged AtPGP1 in transgenic plants. False-color confocal laser scanning microscopy was performed with leaf sections probed with the c-Myc–specific monoclonal antibody 9E10. Detection was achieved with DTAF-conjugated secondary antibody (shown in green). The autofluorescence of chloroplasts is shown in red, whereas the purple color in (Q) and (R) indicates calcofluor white staining of cell walls. (O) and (Q) are transverse sections through cotyledon of a transgenic seedling carrying an ectopically expressed gene encoding c-Myc epitope–tagged AtPGP1. The arrow in (O) indicates the cuticle. (P) and (R) are control sections of wild-type seedlings treated exactly as the sections shown in (O) and (Q). In (O) and (P), bars = 20 μm; in (Q) and (R), bars = 10 μm.
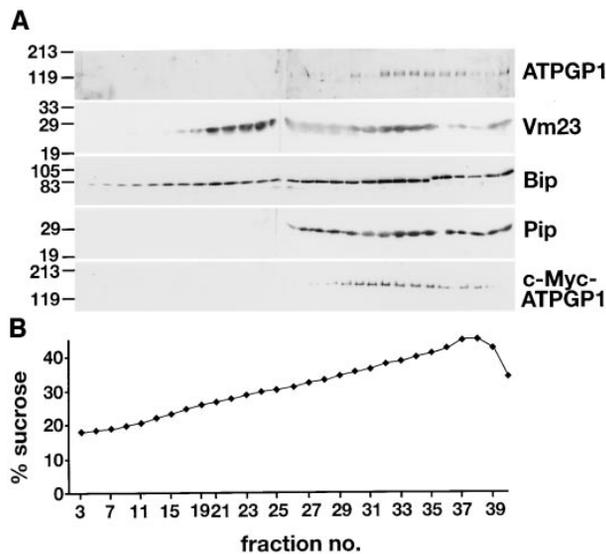co, cotyledon; hy, hypocotyl.

Figure 8. Protein Gel Blot Analysis of Membrane Vesicles Fractionated on Density Gradients.

(A) Membrane vesicles of wild-type Arabidopsis plants and transgenic plants ectopically expressing c-Myc epitope–tagged AtPGP1 were separated simultaneously on continuous sucrose density gradients. Gradients were fractionated, and appropriate aliquots of equal volume were separated on SDS–polyacrylamide gels and blotted. Shown are blots of wild-type samples of a single gradient probed with the AtPGP1-specific polyclonal antiserum or specific antisera to the tonoplast protein VM23, the endoplasmic reticulum protein BiP, and the plasmalemma protein PIP. The blot shown at bottom was prepared with samples derived from transgenic plants ectopically synthesizing c-Myc epitope–tagged AtPGP1 and was probed with the c-Myc epitope–specific monoclonal antibody 9E10. This gradient was run in conjunction with the one containing the wild-type samples, and the distribution of the marker proteins was identical in both gradients (data not shown). Numbers at left indicate the sizes in kilodaltons of marker proteins.
(B) Sucrose concentration of gradient fractions as measured with a refractometer.

that for wild-type function, a threshold level has to be present that was not reached in AS lines.

AtPGP1 Is Involved in a Hypocotyl Elongation Program Active in the Light

The skotomorphogenetic developmental pathway active in darkness is characterized by elongation of the hypocotyl and closed yellow cotyledons that form an apical hook. When exposed to light, seedlings switch from skotomorphogenetic to photomorphogenetic development, which results in inhibition of hypocotyl elongation, opening of the apical hook, unfolding of the cotyledons, and chloroplast development.

Thus, light has an inhibitory effect on hypocotyl cell elongation.

Our experiments showed that within a certain light fluence-rate window, OE plants developed much longer hypocotyls and AS plants distinctly shorter ones than did wild-type plants. Outside of this fluence-rate window, plants of all three genotypes were indistinguishable. We conclude from these results that there exists a hypocotyl elongation program operating at relatively low-light fluence rates in which AtPGP1 is involved and that acts independently of the well-known light-induced hypocotyl elongation inhibition (Koornneef et al., 1980; Kendrick and Kronenberg, 1994). The observed hypocotyl length is the result of the superimposition of these two processes. Because of this superimposition, the light-stimulated hypocotyl elongation is relatively obscured in wild-type plants but is clearly detectable in comparison with AS plants. The fact that relative to the wild type, AS plants exhibited a hypocotyl phenotype opposite to the one observed in OE plants argues that AtPGP1 is involved in the light-stimulated hypocotyl elongation pathway in the wild type.

It turned out that light quantity rather than light quality had a distinct impact on the AtPGP1-mediated hypocotyl phenotype. Although seedlings exposed to continuous blue, red, and far-red light of defined spectra showed the characteristic appearance typical for the particular conditions, the phenotypic difference between the two classes of transgenic plants and the wild type remained qualitatively the same; therefore, it does not seem to depend on a particular range of wavelengths or a specific set of light receptors. This suggests that AtPGP1 acts downstream of a hypothetical point at which the signal transduction pathways of different photoreceptors converge. However, the experiment revealed an interesting result: under dim red light, AtPGP1-mediated hypocotyl elongation in OE seedlings more than compensated for the inhibition of hypocotyl elongation affected by the red light–induced deetiolation, resulting in longer hypocotyls than in etiolated seedlings (Figures 4A and 4B).

Elongation of the hypocotyl is known to be one component of the shade avoidance syndrome, which is induced by light with a low red–to–far-red ratio, because typically it is found under a canopy of dense vegetation (Yanovsky et al., 1995; Smith and Whitelam, 1997; Whitelam and Devlin, 1997). Because in our experiments neutral screens were used to dim white light, it can be ruled out that the observed hypocotyl elongation in the light is part of this syndrome. In addition, the effect would be expected to vanish in the red light experiments, in which this ratio is very high.

The existence of a genetic pathway that regulates Arabidopsis hypocotyl cell elongation in the light has recently also been proposed by Desnos et al. (1996), who described *procuste1* as being a mutant defective in hypocotyl cell elongation in the dark. Although *procuste1* seedlings had short hypocotyls in the dark, they were able to moderately elongate hypocotyls in dim light, thus uncovering a *PROCUSTE1*-independent light-stimulated hypocotyl elongation pathway

referred to as X by Desnos et al. (1996). The AtPGP1-mediated hypocotyl elongation pathway discovered in our experiments and the X pathway may well be identical, because both regulate hypocotyl cell elongation under nonsaturating light conditions in a dose-dependent manner. However, in contrast to Desnos et al. (1996), we observed a moderate increase of hypocotyl elongation with increasing light fluence rates under nonsaturating conditions in the wild type. This may be due to the different ecotypes used by the two groups (ecotype Columbia in the experiments of Desnos et al. [1996] and ecotype RLD in ours) or by differences in experimental conditions.

The Phenotype of Transgenic Plants and the Expression Pattern of *AtPGP1*

Reporter gene constructs and in situ hybridization experiments yielded a consistent *AtPGP1* expression pattern in seedlings. Strong GUS activity was found in the apical regions of both shoots and roots. The only difference was that in reporter plants, the root meristem either was not stained or was not distinctly stained, positioned at the end of a decreasing gradient of GUS activity, whereas in situ hybridization consistently revealed distinct signals in this region. This discrepancy could be explained by assuming lower GUS stability in the region of the quiescent center than in the surrounding tissue or, alternatively, by cross-hybridization of the probe with transcripts of a gene similar to *AtPGP1* that is expressed in this region.

The most surprising fact about the *AtPGP1* expression pattern is that neither GUS activity nor in situ hybridization signals were clearly detected in the hypocotyl itself, indicating that *AtPGP1* may not be expressed in the organ that is affected by antisense-mediated suppression of *AtPGP1* expression (see below). The sections of seedlings 12 hr after germination (shown in Figures 7G and 7H) have been deliberately overstained, resulting in a weak signal in the hypocotyl of the control section hybridized with the sense probe (Figure 7H). The corresponding signal on the section hybridized to the antisense probe is not significantly stronger, in contrast to the signals over the cotyledons. In summary, we were unable to unequivocally detect *AtPGP1* expression in the hypocotyl at any time point during and after germination. However, this does not exclude the possibility that *AtPGP1* gene product is present in hypocotyl cells either as the result of low-level expression during or after germination or as a result of expression during embryogenesis. The *AtPGP1* expression pattern in seedlings, as revealed by reporter plant examination and RNA gel blots, was not detectably altered by different light and other environmental conditions.

The observation that OE plants have longer roots than do wild-type plants is intriguing, considering *AtPGP1* expression in the wild-type root tip. However, because AS plants did not have significantly shorter roots, it is unclear whether the *AtPGP1* gene has a role in a root length regulation path-

way in the wild type. The root phenotype in OE plants may be due to the ectopic nature of *AtPGP1* expression rather than to enhanced expression in root tips. On the other hand, it is possible that AS plants exhibit a root phenotype under other experimental conditions.

After bolting, high GUS activity was associated with the axillary meristematic regions and adjacent tissue, including the phloem and parenchyma in the basal regions of stem leaves. In flowers, the receptacle was the only part that in some lines (six of 13) showed GUS activity. The activity persisted until silique development was completed. This late activity may reflect stability of the enzyme rather than persisting synthesis. No phenotypic effect of the manipulation of *AtPGP1* expression was discovered in transgenic plants after the seedling stage.

How May AtPGP1 Affect Hypocotyl Cell Length?

Hypocotyl cells respond directly or indirectly to diverse environmental stimuli such as wavelength composition, fluence rate, and direction of the incident light. In some cases, perception and signaling may be cell autonomous (Neuhaus et al., 1993); otherwise, sites of perception and of action are apart in separate cells. Therefore, signals have to emanate from the site of perception to regulate directly or indirectly the length of the hypocotyl cells appropriately. An attractive hypothesis is that the AtPGP1 protein is involved in the transport of such a signal. A conceivable function of AtPGP1 would therefore be the export of a hormone-like compound from the shoot apical region that would regulate hypocotyl cell length. The production of this compound would be under the control of the light fluence rate perceived by the cotyledons and possibly other, yet unknown factors, whereas its export would be mediated by the constitutive AtPGP1 exporter. If the distribution of AtPGP1 is indeed confined to the apical regions, as suggested by our data, then the AtPGP1-exported signal would have to reach hypocotyl cells by diffusion into the apoplast or by transport through the vascular strand to induce cell expansion in competent cells. This signal is unlikely to be one of the basic plant hormones, because if it were, one would expect that constitutive ectopic expression of *AtPGP1* would have greater phenotypic consequences than those that have been observed. Alternatively, if AtPGP1 transporter is present in the plasmalemma of hypocotyl cells, it may be involved in the import of an incoming signal molecule, although, with the exception of the bacterial periplasmic binding protein–dependent importers, all ABC transporters analyzed have been reported to function in an export process (Higgins, 1992).

One conceivable hypothesis is that the substrate of the AtPGP1 exporter is a peptide hormone. MDR-like transporters have been shown to provide an export mechanism for peptides that is independent of the classic N-terminal transit sequence, as, for example, in yeast, in which the STE6 transporter is involved in the secretion of the 12-amino-acid-long

a-mating-type pheromone (Kuchler et al., 1989; McGrath and Varshavsky, 1989), or in mammals, in which the MDR-like TAP1/TAP2 complex transports processed antigens into the endoplasmic reticulum for assembly with major histocompatibility complex class I proteins (Williams et al., 1996). In plants, two prominent hormone-like peptides, systemin and early nodulin ENOD40, have been described (McGurl et al., 1992; van de Sande et al., 1996). Both lack a hydrophobic leader peptide in the active form as well as during their synthesis, but they are still exported out of cells, conceivably by ABC transporters.

There is increasing evidence that a variety of cellular processes, among them defense responses, growth, and development, are mediated by small peptides serving as signaling molecules (Pearce et al., 1991; McGurl et al., 1992; Matsubayashi and Sakagami, 1996; van de Sande et al., 1996; John et al., 1997; Miklashevichs et al., 1997). Although one can only speculate on the mechanism mediating hypocotyl cell elongation in the light at present, our results implicate a transmembrane transport function in this regulatory pathway. The identification of the substrate that is translocated by AtPGP1 will help us to understand this pathway, and this task should be facilitated by the transgenic plants described.

METHODS

Plant Growth Conditions

Arabidopsis thaliana ecotype RLD (stock No. N913; Arabidopsis Stock Centre, Nottingham, UK) was grown on Florabella cactus soil (Klasmann/Deilmann, Geeste, Germany) in a growth chamber (18 hr of light and 6 hr of darkness at 24°C) after a 4-day vernalization period (4°C in dim light) by using Arasystem containers (Lehle Seeds, Round Rock, TX). For growth under sterile conditions, seeds were surface sterilized (5 min in 70% ethanol, followed by a 15-min incubation in 5% [v/v] sodium hypochlorite, 0.2% [v/v] Tween 20, and a threefold rinse in sterile distilled water) and sown on half-strength Murashige and Skoog (MS) salts (Sigma) supplemented with 1% sucrose, $1 \times$ Gamborg's vitamins, 0.5 g/L Mes, pH 5.7, and 0.8% (w/v) phytagar (Gibco BRL) in Petri dishes.

Light Conditions

White Light

Biolux fluorescent tubes (Osram, Munich, Germany) were used as sources for white light.

Red Light

The light of seven white fluorescence tubes (warm white, model L20 W/30 S; Osram) was filtered through 3 mm of red Plexiglas (red No.

501; Röhm and Haas, Darmstadt, Germany), resulting in a spectrum with a peak at 610 nm and a half bandwidth of $\sim$60 nm.

Blue Light

The light of seven blue fluorescent tubes (No. 8531; Philips, Eindhoven, The Netherlands) was filtered through a Plexiglas screen (blue No. 627; Röhm and Haas) to give a peak at 455 nm with a half bandwidth of 30 nm.

Far-Red Light

The light from 10 light bulbs (Centra; Osram) was filtered through a combination of red (3 mm, No. 501) and blue (6 mm, No. 627) Plexiglas to obtain a far-red spectrum with a cutoff below 710 nm, reaching a maximum at 750 nm. Cheesecloth and a white mesh were used as neutral screens to dim the light. The individual fluence rates were obtained by moving the plants vertically closer to or away from the light source. The light fluence-rate was measured with a quantum sensor (model Li-190SB; Li-Cor, Lincoln, NE). All wavelengths and spectra were controlled with a Li-Cor spectroradiometer (model Li-1800).

Test for Resistance to Toxic Agents

Plants were grown for up to 3 weeks in liquid MS medium supplemented with test agents on a rotary shaker at 90 rpm. The herbicides atrazine (Novartis AG, Basel, Switzerland), azifluorfen (Rhône-Poulenc Rorer GmbH, Cologne, Germany), and paraquat (Chevron Chemical Co., San Francisco, CA) were tested in a range of 0.01 to 0.05 µg/mL; alachlor (Monsanto, St. Louis, MO) was tested in a range of 0.05 to 0.5 µg/mL. The drugs doxorubicine (Sigma) and emetine (Sigma) were applied at a concentration range of 0.1 to 100 µg/mL.

Measurement of Hypocotyl and Root Length

Seedlings were fixed in 70% ethanol and spread on agar plates. The plates were scanned on a flatbed scanner, and hypocotyl lengths were determined on the digitized image with the help of a standard using the National Institutes of Health (Bethesda, MD) Image software package (Macintosh version 1.60). To determine the root length of soil-grown plantlets, we removed the pot and suspended the soil containing the plantlets in water to clean the seedlings. Seedlings with intact roots were processed as described above.

Determination of Hypocotyl Cell Numbers and Scanning Electron Microscopy

Seedlings were cleared by incubation for 24 hr in a chloral hydrate–H_2O mixture (2.5:1), and the number of cells per file was determined under a microscope. For scanning electron microscopy, seedlings were fixed for 24 hr in a solution containing 4% formaldehyde, 50% acetone, and 5% acetic acid. After dehydration in 100% acetone, critical point drying, and coating with gold, they were analyzed with a scanning electron microscope (model S-4100; Hitachi, Yokohama, Japan).

Construction of Transformation Plasmids

GUS *Reporter Construct*

The starting plasmid was a 4-kb PstI fragment in pBluescript SK+ (Stratagene, La Jolla, CA) containing the 5′ part of the *AtPGP1* gene, including ~2.1 kb of the 5′ flanking region (Dudler and Hertig, 1992). From this plasmid, a 2.1-kb promoter fragment was cut out with HindIII (which cleaves in the multiple cloning site on the upstream side) and BclI (cutting in the leader region ~12 bp downstream of the transcriptional initiation site in the *AtPGP1* gene [nucleotide position 804; Dudler and Hertig, 1992]) and cloned between the HindIII and BamHI sites of the multiple cloning site of the plant transformation vector pBI101 (Clontech, Palo Alto, CA) upstream of the *GUS* gene.

Overexpression Construct

The starting plasmid was the one used for the *GUS* reporter construct. The 2.1-kb *AtPGP1* promoter fragment was cut out with AccI. AccI cuts in the multiple cloning site on the upstream side of the 4-kb PstI fragment and in the leader region ~25 bp downstream of the transcriptional initiation site in the *AtPGP1* gene (nucleotide position 817; Dudler and Hertig, 1992) and was replaced with a synthetic double-stranded oligonucleotide containing a BamHI restriction site (upper strand, 5′-CGTGGGATCC; lower strand, 5′-CTGGATCCCA). The upstream PstI site in the polylinker was lost during this manipulation. Thus, the 5-kb PstI fragment containing the rest of the *AtPGP1* gene and 3′ flanking sequences (Dudler and Hertig, 1992) could be cloned into the remaining downstream PstI site of this plasmid.

One of the resulting plasmids with the correct orientation of the 5-kb PstI fragment was selected and named pOE. The complete but promoterless 7-kb *AtPGP1* gene was cut out from pOE with BamHI, which cleaves in the newly introduced oligonucleotide and in the multiple cloning site downstream of the insert. The 7-kb BamHI fragment was inserted into the BamHI cloning site of the plant transformation vector pBI121 (Clontech), from which the *GUS* gene had been deleted previously by digestion with SmaI and SacI, with religation of the vector fragment after blunting the SacI end with T4 DNA polymerase. One of the resulting plasmids with the correct orientation of the *AtPGP1* gene relative to the cauliflower mosaic virus (CaMV) 35S promoter of the modified pBI121 vector was selected for plant transformation and named pBIMDR1.

Antisense Construct

The antisense construct contained the first 1.9 kb from the 5′ end of an *AtPGP1* cDNA in an antisense orientation between the CaMV 35S promoter and the nopaline synthase gene termination sequences of pBI121. The cDNA fragment was obtained using the reverse transcriptase–polymerase chain reaction procedure, as described by Dudler and Hertig (1992). Briefly, the 1.9-kb cDNA was amplified in three slightly overlapping pieces by using the first three primer pairs, as indicated in Figure 2 of Dudler and Hertig (1992). All primers had additional nucleotides at the 5′ ends to give suitable restriction sites for cloning of the resulting fragments. Thus, the most upstream piece of ~320 bp was flanked by SacI (5′) and XbaI (3′) sites; the slightly overlapping middle piece of ~680 bp had a SacI (5′) site and an XbaI (3′) site; and the most downstream piece of ~890 bp, which slightly overlapped with the middle fragment, was flanked by XbaI (5′) and BamHI (3′) sites.

These fragments were each cloned into pBluescript SK+ to yield pMDRPCR1 (upstream fragment), pMDRPCR2 (middle fragment), and pMDRPCR3 (downstream fragment). pMDRPCR1 and pMDRPCR2 contained a unique NcoI site in the part at which they overlapped (nucleotide position 1097; Dudler and Hertig, 1992). Thus, the short NcoI-XbaI fragment of pMDRPCR1 was replaced with the NcoI-XbaI fragment of pMDRPCR2 to give pMDRPCR12. The XbaI-BamHI insert of pMDRPCR3 was then cloned into pMDRPCR12. Because the XbaI sites of the two plasmids were at identical positions relative to the gene sequence (which contains five of the six nucleotides of the recognition sequence), the resulting plasmid (pMDRPCR123) contained 1.9 kb of cDNA sequences identical to the exon sequences of *AtPGP1*, except for the one-nucleotide change (T instead of a G residue at position 2037; Dudler and Hertig, 1992) that resulted in the XbaI site. The 1.9-kb insert of pMDRPCR123 was cut out with SacI and BamHI and used to replace the *GUS* gene of pBI121, resulting in pBIAS1.9.

c-Myc AtPGP1 Construct

A synthetic double-stranded oligonucleotide with AatII-compatible sticky ends (top strand, 5′-AGAGCAGAAGCTTATCTCCGAGGA-GGACCTTACGT; bottom strand, 5′-AAGGTCCTCCTCGGAGATAAG-CTTCTGCTCTAACGT) encoding the c-Myc epitope EQKLISEEDL (Evan et al., 1985) was designed for ligation into the AatII site of pOE (see above) at nucleotide position 5789 of the *AtPGP1* gene (Dudler and Hertig, 1992). The c-Myc epitope is thereby inserted at amino acid 1274 of the 1286–amino acid protein. The resulting clones were sequenced, and one with the insert in the correct orientation was selected and named pOEmyc. The modified *AtPGP1* gene was cut out from pOEmyc with BamHI and inserted into the BamHI cloning site of the plant transformation vector pBI121 from which the *GUS* gene had been previously deleted, as described above. One of the resulting plasmids with the correct orientation of the insert relative to the CaMV 35S promoter was selected for plant transformation and named pBIMDRMyc1.

Generation of AtPGP1-Specific Antiserum

A 613-bp BglII-HindIII fragment derived from pMDRPCR3 (see *Antisense Construct*, above) was cloned into the corresponding restriction sites of the bacterial expression vector p6xHis-DHFRS(−2) (Stüber et al., 1990). The resulting plasmid permitted isopropyl β-D-thiogalacto-pyranoside–inducible expression in *Escherichia coli* of a fusion protein consisting of an N-terminal histidine hexamer followed by a derivative of the mouse dihydrofolate reductase fused to part of the AtPGP1 protein (amino acids 340 to 544) that contained the first ATP binding domain. The fusion protein was purified from *E. coli* lysates by nickel chelate affinity chromatography using its histidine affinity tag, according to Stüber et al. (1990). The eluted protein was further subjected to SDS-PAGE. After Coomassie Brilliant Blue R 250 staining, the gel slice containing the fusion protein was cut out, crushed, and directly used to immunize rabbits. Immunization and preparation of antiserum were performed by Eurogentec (Seraing, Belgium).

Plant Transformation and Selection

Plant transformation plasmids were electroporated into *Agrobacterium tumefaciens* GV3101 (Van Larebeke et al., 1974) as described

by Wen-jun and Forde (1989). The in-the-plant Agrobacterium-mediated transformation by vacuum infiltration was used as described previously (Bechtold et al., 1993), with the following modifications. Plants were infiltrated for 20 min without using a vacuum, and the infiltration medium (2.3 g/L MS salts, 0.112 g/L Gamborg's B5 vitamins, 0.5 g/L Mes, 5% [w/v] sucrose, and 0.044 μM 6-benzylaminopurine) contained 0.03% Silwet L-77 (Union Carbide Corp., Danbury, CT). T_1 seeds were collected, dried at 29°C, and sown on sterile media containing 50 μg/mL kanamycin to select the transformants. Surviving T_1 plantlets were transferred to soil to set seeds (T_2). The segregation frequency of the T_2 generation with regard to kanamycin resistance was determined on selective media. Seeds (T_3) of transgenic lines segregating for kanamycin resistance in a Mendelian ratio of 3:1 typical for a single integration locus were collected and again sown on selective media. T_2 plants were assumed to be homozygous for the transgene if all of 50 to 150 progeny seedlings were kanamycin resistant.

RNA Extraction and Gel Blot Analysis

After homogenizing plant tissue in liquid nitrogen with a mortar and pestle, we prepared total RNA by the hot phenol method and LiCl precipitation, as described previously (Dudler and Hertig, 1992). RNA gel blot preparation and hybridization were performed according to standard procedures (Maniatis et al., 1982). The ^{32}P-labeled 1.9-kb insert of pMDRPCR123 was used as a probe.

Protein Extraction and Gel Blot Analysis

Arabidopsis tissue was homogenized in 3 volumes of homogenization buffer (50 mM Hepes-KOH, pH 7.5, 5 mM EDTA, 0.1% BSA, 1 mM phenylmethylsulfonyl fluoride, 2 mM DTT, 1% [w/v] polyvinylpolypyrrolidone, 0.1 mg/mL butylated hydroxytoluene, and 0.25 M sucrose) in a Waring blender, filtered through two layers of cheesecloth, and centrifuged at 7000g for 15 min to remove debris. The microsomal membrane fraction was pelleted from the supernatant by ultracentrifugation at 100,000g for 30 min. The pellet was resuspended in a buffer containing 5 mM Tris-HCl, pH 7, 2 mM EDTA, and 250 mM sucrose with the aid of a Potter homogenizer (Huber, Reinach, Switzerland). Protein concentrations were determined using the Bio-Rad protein assay. Aliquots were denatured by the addition of a 0.25 volume of 5 $\times$ sample buffer (60 mM Tris-HCl, pH 6.8, 15% SDS, 25% glycerol, 5% β-mercaptoethanol, and 0.1% bromophenol blue), incubation at 60°C for 15 min, and sonication for another 15 min in a sonication water bath (47 kHz; Bransonic, Aasoest, The Netherlands). It was of crucial importance that the membrane vesicles were denatured in the largest possible volume; otherwise, AtPGP1 did not enter the separating gel.

Proteins were separated on 7% SDS–polyacrylamide gels and transferred to nitrocellulose filters (0.45-μm pore size; Millipore, Bedford, MA) by using a semidry blotting apparatus (Pharmacia-LKB, Uppsala, Sweden). For immunodetection of AtPGP1, the blots were blocked in TBS (20 mM Tris-HCl, pH 7.5, 137 mM NaCl, and 0.1% [v/v] Tween 20) containing 7.5% (w/v) nonfat dry milk powder and incubated in a 1:1000 dilution of anti-AtPGP1 antiserum. Blots were washed, incubated with goat anti–rabbit horseradish peroxidase–conjugated secondary antibody, and developed using a chemiluminescent immunodetection system (ECL; Amersham International) according to the manufacturer's directions. Milk powder was included

in all incubation steps and washes except the last wash before the addition of the detection substrate.

For densitometric analysis, the autoradiogram of the gel blot was scanned with a flatbed scanner, and the resulting image was processed with the National Institutes of Health Image software package (Macintosh version 1.60), which allowed integration and quantification of signals.

Density Gradient Fractionation of Membrane Vesicles

The microsomal membrane fraction was isolated as described above, but the vesicles were resuspended in gradient buffer (10 mM Tris-Mes, pH 7.0, 1 mM DTT, and 0.1 mM phenylmethanesulfonyl fluoride) containing 250 mM sucrose. A continuous gradient from 15 to 45% (w/v) sucrose in gradient buffer was poured with the aid of a gradient former (Auto Density Flow II; Buchler Instruments, Fort Lee, NJ). After ultracentrifugation at 49,000 rpm for 6 hr in a TV 850 rotor (Sorvall, Newtown, CT), gradient fractions were collected, and 0.2 mL of 5 $\times$ sample buffer was added to each 0.8-mL fraction. Fractions were frozen in liquid nitrogen and stored at −80°C until used. Protein gel electrophoresis, blotting, and immunodetection of AtPGP1 were performed as described above. To detect c-Myc–tagged AtPGP1, monoclonal antibody 9E10 (1:1000; Calbiochem, La Jolla, CA) and horseradish peroxidase–conjugated goat anti–mouse secondary antibody (1:3000; Bio-Rad) were used. The antibodies against marker proteins were a gift of A.R. Schäffner, Ludwid-Maximilian University, Munich, Germany (chicken anti-PIP; Kammerloher et al., 1994), M. Chrispeels, University of California, San Diego (rabbit anti-BiP), and M. Maeshima, Institute of Low Temperature Science, Hokkaido University, Sapporo, Japan (rabbit anti-VM23; Maeshima, 1992). The antisera were used at a dilution of 1:1000, and detection was achieved with a 1:3000 dilution of the corresponding specific horseradish peroxidase–coupled secondary antibody (Bio-Rad) and the ECL chemiluminescent detection system (Amersham International).

Histochemical GUS Staining

Histochemical detection of GUS activity was performed with whole seedlings or plant parts. As negative controls, untransformed plants were used. Tissue was vacuum infiltrated for 2 min with fixing solution (0.01% Silwet L77 detergent [Union Carbide Corp.], 0.3% formaldehyde, 10 mM Mes, pH 6.5, and 0.3 M mannitol) and incubated for 45 min at room temperature. After washing three times in 50 mM NaPO$_4$, pH 7, the tissue was incubated in the same buffer containing 1 mM 5-bromo-4-chloro-3-indolyl β-D-glucuronic acid at 37°C for 16 hr. Chlorophyll was then eluted by incubation in 70% ethanol at 37°C.

In Situ Hybridization

Digoxigenin-labeled sense and antisense RNA probes were synthesized using the digoxigenin RNA labeling kit (Boehringer Mannheim).The template was pMDRPCR4, a pBluescript SK+ vector containing a 1080-bp-long partial *AtPGP1* cDNA amplified by a reverse transcriptase–polymerase chain reaction procedure that covered part of exon 8, exon 9, and part of exon 10 (from positions 3418 to 4657 in Figure 1 of Dudler and Hertig [1992]). In situ hybridization to 8-μm-thick Paraplast (Sigma) sections of 3- to 5-day-old formaldehyde-fixed Arabidopsis seedlings was performed according to Jackson

(1991), with the modifications described by Lincoln et al. (1994). Riboprobes were used at a concentration of ~0.6 ng/μL. Whole-mount in situ hybridization was performed with roots of 3- to 5-day-old seedlings of Arabidopsis according to Tautz and Pfeifle (1989) and exactly as described by Ludevid et al. (1992).

Tissue Sections and Immunohistochemistry

Seeds were germinated and grown submerged in liquid MS medium at 24°C on a rotary shaker at 90 rpm for 10 to 14 days. Leaves and stems were placed on a slice of polystyrol, and sections were cut by hand as thin as possible with a razor blade. Sections were immediately transferred to microtiter plates and fixed with pFA fixative (3.5% p-formaldehyde, 50 mM sucrose, 0.01% Silwet L-77, and 90 mM sodium phosphate, pH 6.8) for at least 3 hr at room temperature. Sections were washed for 30 min and then twice for 10 min in washing buffer (90 mM sodium phosphate and 0.2% glycine, pH 7.2), incubated in blocking buffer (150 mM NaCl, 1.5% [w/v] BSA, 0.03% [w/v] NaN$_3$, and 50 mM sodium phosphate, pH 7.5) overnight at 4°C, and finally incubated with a 1:3000 dilution of the monoclonal antibody 9E10 (Calbiochem) in blocking buffer for 24 hr at 4°C. The tissue sections were then washed twice for 15 min with blocking buffer and incubated in a 1:150 dilution of dichlorotriazynil aminofluorescein (DTAF)–coupled goat anti–mouse IgG secondary antibody (Jackson Immuno Research Laboratories, West Grove, PA) in blocking buffer. All following steps were conducted under light-tight conditions. After an incubation period of 18 to 24 hr at 4°C, sections were washed twice with blocking buffer and once with 90 mM sodium phosphate, pH 7.5. For nuclear staining, sections were incubated in 3 μg/mL 4′,6-diamidino-2-phenylindole (Sigma) in 90 mM sodium phosphate, pH 7.5, for 45 min. Cell walls were stained with 0.02% (w/v) calcofluor white M2R (Sigma) in 90 mM sodium phosphate, pH 7.5, for 5 min. Finally, the sections were rinsed once in 90 mM sodium phosphate, pH 7.5, and incubated for 5 min in mounting solution (50% glycerol, 0.02% p-phenylenediamine, 75 mM NaCl, and 50 mM Tris-HCl, pH 8) before being mounted on a microscope slide and covered with a coverslip, the edges of which were sealed with nail polish.

The sections were examined with an inverted confocal laser scanning microscope (Leica, Heidelberg, Germany) equipped with the appropriate filter sets (BP 522/32-FITC [Leica] for DTAF, LP 590 nm [Leica] for the autofluorescence of chloroplasts, and BP 455/30-DAPI [Leica] for DAPI and calcofluor white M2R). Fluorescence images of the separate channels were digitized with the Leica Scanware software and merged by using Adobe Photoshop version 4.0 (Adobe Systems Inc., San Jose, CA).

REFERENCES

Bechtold, N., Ellis, J., and Pelletier, G. (1993). *In planta Agrobacterium*-mediated gene transfer by infiltration of adult *Arabidopsis thaliana* plants. C. R. Acad. Sci. Ser. III Sci. Vie **316,** 1194–1199.

Chamovitz, D.A., and Deng, X.W. (1995). The novel components of the Arabidopsis light signaling pathway may define a group of general developmental regulators shared by both animal and plant kingdoms. Cell **82,** 353–354.

Desnos, T., Orbovic, V., Bellini, C., Kronenberger, J., Caboche, M., Traas, J., and Höfte, H. (1996). *procuste1* mutants identify two distinct genetic pathways controlling hypocotyl cell elongation, respectively in dark- and light-grown *Arabidopsis* seedlings. Development **122,** 683–693.

Dudler, R., and Hertig, C. (1992). Structure of an *mdr*-like gene from *Arabidopsis thaliana*: Evolutionary implications. J. Biol. Chem. **267,** 5882–5888.

Evan, G.I., Lewis, G.K., Ramsay, G., and Bishop, J.M. (1985). Isolation of monoclonal antibodies specific for human c-*myc* proto-oncogene product. Mol. Cell. Biol. **5,** 3610–3616.

Gendreau, E., Traas, J., Desnos, T., Grandjean, O., Caboche, M., and Höfte, H. (1997). Cellular basis of hypocotyl growth in *Arabidopsis thaliana.* Plant Physiol. **114,** 295–305.

Golan, A., Tepper, M., Soudry, E., Horwitz, B.A., and Gepstein, S. (1996). Cytokinin, acting through ethylene, restores gravitropism to Arabidopsis seedlings grown under red light. Plant Physiol. **112,** 901–904.

Gottesman, M.M., Hrycyna, C.A., Schoenlein, P.V., Germann, U.A., and Pastan, I. (1995). Genetic analysis of the multidrug transporter. Annu. Rev. Genet. **29,** 607–649.

Gottesman, M.M., Pastan, I., and Ambudkar, S.V. (1996). P-Glycoprotein and multidrug resistance. Curr. Opin. Gen. Dev. **6,** 610–617.

Herman, E.M., Li, X., Su, R.T., Larsen, P., Hsu, H., and Sze, H. (1994). Vacuolar-type H$^+$-ATPases are associated with the endoplasmatic reticulum and provacuoles of root tip cells. Plant Physiol. **106,** 1313–1324.

Higgins, C.F. (1992). ABC transporters: From microorganisms to man. Annu. Rev. Cell Biol. **8,** 67–113.

Jackson, D. (1991). In situ hybridization in plants. In Molecular Plant Pathology: A Practical Approach, D.J. Bowles, S.J. Gurr, and M. McPherson, eds (Oxford, UK: Oxford University Press), pp. 163–174.

John, M., Schmidt, J., Walden, R., Czaja, I., Dulz, M., Schell, J., and Rohrig, H. (1997). Lipochitooligosaccharide-induced tobacco cells release a peptide as mediator of the glycolipid signal. Proc. Natl. Acad. Sci. USA **94,** 10178–10182.

Kammerloher, W., Fischer, U., Piechottka, G.P., and Schäffner, A.R. (1994). Water channels in the plant plasma membrane cloned by immunoselection from a mammalian expression system. Plant J. **6,** 187–199.

Kendrick, R.E., and Kronenberg, G.M.H. (1994). Photomorphogenesis in Plants. (Dordrecht, The Netherlands: Kluwer Academic Publishers).

Koornneef, M., Rolff, E., and Spruit, C.J.P. (1980). Genetic control of light inhibited hypocotyl elongation in *Arabidopsis thaliana.* Int. J. Plant Physiol. **100,** 147–160.

Kuchler, K., Sterne, R.E., and Thorner, J. (1989). *Saccharomyces cerevisiae STE6* gene product: A novel pathway for protein export in eukaryotic cells. EMBO J. **8,** 3973–3984.

Lincoln, C., Long, J., Yamaguchi, J., Serikawa, K., and Hake, S. (1994). A *knotted1*-like homeobox gene in Arabidopsis is expressed in the vegetative meristem and dramatically alters leaf morphology when overexpressed in transgenic plants. Plant Cell **6,** 1859–1876.

Ludevid, D., Höfte, H., Himelblau, E., and Chrispeels, M.J. (1992). The expression pattern of the tonoplast intrinsic protein α-TIP in *Arabidopsis thaliana* is correlated with cell enlargement. Plant Physiol. **100,** 1633–1639.

Maeshima, M. (1992). Characterization of the major integral protein of vacuolar membrane. Plant Physiol. **98,** 1248–1254.

Maniatis, T., Fritsch, E.F., and Sambrook, J. (1982). Molecular Cloning: A Laboratory Manual. (Cold Spring Harbor, NY: Cold Spring Harbor Laboratory Press).

Matsubayashi, Y., and Sakagami, Y. (1996). Phytosulfokines, sulfated peptides that induce the proliferation of single mesophyll cells of *Asparagus officinalis* L. Proc. Natl. Acad. Sci. USA **93,** 7623–7627.

McGrath, J.P., and Varshavsky, A. (1989). The yeast *STE6* gene encodes a homologue of the mammalian multidrug resistance P-glycoprotein. Nature **340,** 400–404.

McGurl, B., Pearce, G., Orozco-Cardenas, M., and Ryan, C.A. (1992). Structure, expression, and antisense inhibition of the systemin precursor gene. Science **255,** 1570–1573.

Miklashevichs, E., Czaja, I., Cordeiro, A., Prinsen, E., Schell, J., and Walden, R. (1997). T-DNA tagging reveals a novel cDNA triggering cytokinin- and auxin-independent protoplast division. Plant J. **12,** 489–498.

Neuhaus, G., Bowler, C., Kern, R., and Chua, N.-H. (1993). Calcium-calmodulin-dependent and independent phytochrome signal transduction pathways. Cell **73,** 937–952.

Ortiz, D.F., Kreppel, L., Speiser, D.M., Scheel, G., McDonald, G., and Ow, D.W. (1992). Heavy metal tolerance in the fission yeast requires an ATP-binding cassette-type vacuolar membrane transporter. EMBO J. **11,** 3491–3499.

Pearce, G., Strydom, D., Johnson, S., and Ryan, C.A. (1991). A polypeptide from tomato leaves induces wound-inducible proteinase inhibitor proteins. Science **253,** 895–898.

Quail, P.H., Boylan, M.T., Parks, B.M., Short, T.W., Xu, Y., and Wagner, D. (1995). Phytochromes: Photosensory perception and signal transduction. Science **268,** 675–680.

Smith, H., and Whitelam, G.C. (1997). The shade avoidance syndrome—Multiple responses mediated by multiple phytochromes. Plant Cell Environ. **20,** 840–844.

Stüber, D., Matile, H., and Garotta, G. (1990). System for high-level production in *Escherichia coli* and rapid purification of recombinant proteins: Applications to epitope mapping, preparation of antibodies, and structure–function analysis. In Immunological Methods, I. Levkovits and B. Pernis, eds (New York: Academic Press), pp. 121–152.

Tautz, D., and Pfeifle, C. (1989). A non-radioactive in situ hybridization method for the localization of specific RNAs in *Drosophila* embryos reveals translational control of the segmentation gene *hunchback.* Chromosoma **98,** 81–85.

van de Sande, K., Pawlowski, K., Czaja, I., Wieneke, U., Schell, J., Schmidt, J., Walden, R., Matvienko, M., Wellink, J., van Kammen, A., Franssen, H., and Bisseling, T. (1996). Modification of phytohormone response by a peptide encoded by *ENOD40* of legumes and a nonlegume. Science **273,** 370–373.

Van Larebeke, N., Engler, G., Holsters, M., Van den Elscker, S., Zainen, I., Schilperoort, R.A., and Schell, J. (1974). Large plasmid in *Agrobacterium tumefaciens* essential for crown gall–inducing ability. Nature **252,** 169–170.

von Arnim, A.G., and Deng, X.W. (1994). Light inactivation of Arabidopsis photomorphogenic repressor COP1 involves a cell-specific regulation of its nucleocytoplasmic partitioning. Cell **79,** 1035–1045.

Wen-jun, S., and Forde, B.G. (1989). Efficient transformation of *Agrobacterium* spp. by high voltage electroporation. Nucleic Acids Res. **17,** 8358–8359.

Whitelam, G.C., and Devlin, P.F. (1997). Roles of different phytochromes in *Arabidopsis* photomorphogenesis. Plant Cell Environ. **20,** 752–758.

Williams, D.B., Vsilakos, A., and Suh, W. (1996). Peptide presentation by MHC class I molecules. Trends Cell Biol. **6,** 267–273.

Yanovsky, M.J., Casal, J.J., and Whitelam, G.C. (1995). Phytochrome A, phytochrome B and HY4 are involved in hypocotyl growth responses to natural radiation in *Arabidopsis*: Weak deetiolation of the *phyA* mutant under dense canopies. Plant Cell Environ. **18,** 788–794.

Involvement of an ABC Transporter in a Developmental Pathway Regulating Hypocotyl Cell Elongation in the Light

Michael Sidler, Paul Hassa, Sameez Hasan, Christoph Ringli and Robert Dudler

This information is current as of January 15, 2021

References	This article cites 33 articles, 15 of which can be accessed free at: /content/10/10/1623.full.html#ref-list-1
Permissions	https://www.copyright.com/ccc/openurl.do?sid=pd_hw1532298X&issn=1532298X&WT.mc_id=pd_hw1532298X
eTOCs	Sign up for eTOCs at: http://www.plantcell.org/cgi/alerts/ctmain
CiteTrack Alerts	Sign up for CiteTrack Alerts at: http://www.plantcell.org/cgi/alerts/ctmain
Subscription Information	Subscription Information for *The Plant Cell* and *Plant Physiology* is available at: http://www.aspb.org/publications/subscriptions.cfm